

FILM COOLING PERFORMANCE USING TRANSIENT LIQUID CRYSTALS MEASUREMENTS

EHAB RADWAN¹, M. F. ABDRABBO² & M. G. A. HIGAZY³

¹PhD Student, Shoubra Faculty of Engineering, Benha University, Egypt, Cairo

^{2,3}Shoubra Faculty of Engineering, Benha University, Egypt, Cairo

ABSTRACT

This paper is an experimental investigation of the film cooling performance over a flat plate using transient liquid crystal measurements. Cylindrical hole with straight angle injection was used. Experiments were conducted at different blowing ratio ($M=0.5$ to 1.5) and different cooling channel Reynolds number ($Re_{Dh,c}=10000$, to $Re_{Dh,c}=40000$). All Experiments were conducted at constant hot gas Reynolds number and constant pressure ratio and. Film cooling Performance h (heat transfer coefficient) and η (adiabatic film cooling effectiveness are determined using the transient liquid crystal method combined with a numerical regression method to solve for the two unknowns). The results are discussed and compared to previously published literature.

KEYWORDS: Adiabatic, Film Cooling, Heat Transfer, Transient, Liquid Crystal

NOMENCLATURES

Abbreviations

CHSA	Cylindrical hole straight angle
ETA	Program for results calculations
ILS	Integral length scale
LFE	Laminar Flow Element
PROTEIN	Program for video color analysis
RTD	Resistance Thermometer Device
TLC	Thermochromics liquid crystal
VFM	vortex flow meter

Latin Letters

D	Cooling hole diameter
Dh	Hydraulic diameter
DR	Density ratio
h	Convective Heat Transfer
I	Momentum Flux Ratio,

k	Thermal Conductivity
L	Cooling hole length
M	Blowing ratio,
m	Mass flow rate
Re	Reynolds number
t	Time
q _w	Wall heat flux
X	Stream-wise coordinate
Y	Lateral coordinate
Z	Direction normal to the surface

Greek Letters

α	Hole inclination angle
α_r	Rib angle
β	Hole compound angle
δ	Boundary layer thickness
η	Film cooling effective-ness
τ	Time step
ξ	wall thickness
ρ	Density of plate

Subscripts

0	Without film cooling
aw	Adiabatic wall
c	Cooling channel
h	Hot gas channel
i	Initial
jet	Film-cooling air jet
st	Static
w	Wall

INTRODUCTION

In a modern gas turbine, the Turbine inlet temperature has increased to more than 1200° C in the middle of the last century, so the cooling of gas turbine blades has become necessary. Film cooling is a most effective and reliable method to avoid burning of highly loaded gas turbine blades. Early work on film cooling has first been investigated by [1],[2], and [3] also resumed work on cooling hole shape. A review of calculation methods for the heat transfer in film cooling systems in comparison with experimental results is outlined in [4]. The quality of the cooling is characterized by two parameters, the heat transfer coefficient h on the outer surface, and the film cooling effectiveness η_{aw} . Research on film cooling focuses mainly on influencing parameters, as Influencing parameters on the hot outer surface (e.g.: δ , Red, geometry), Cooling hole geometry (e.g.L/d, hole shape), The approaching flow from the internal cooling channel (e.g.Re_{Dh}, M, Flow pattern), and measurement technique. The following brief literature reviews both the film cooling performance and Transient liquid crystal measurement technique. [5] Have investigated the vortex structure of the jets in a cross flow experimentally. The interaction of the coolant jet and cross flow results in the formation of a pair of counter-rotating vortices, or kidney vortices. The rotation is such that hot air is forced down beneath the jet to the blade wall and the vortices tend to lift the jet of the surface. The introduction of a counter-rotating vortex pair weakens this effect by cancellation [6]. The coolant flow pattern for a cooling hole geometry $L/d < 5$ has an important effect [7]. [8] Showed a significant influence of the cooling channel direction on the film cooling performance. Further studies of [9] and [10] proved the influence of the coolant flow pattern on the film cooling. [11] Proposed a patent for cooling flow guidance, structure, reducing the vortex production. [12] Investigated the flow physics of straight film cooling holes numerically.

TRANSIENT MEASUREMENT TECHNIQUE

The transient measurement technique has been shown to be beneficial for heat transfer measurements, since it can be performed quickly and simultaneously and provides very accurate results. The reaction of the wall temperature is examined for a change in the fluid temperature. For this purpose, starting from an equilibrium state, in which the complete measuring system is at a constant homogeneous temperature, a sudden increase in temperature initiates the mainstream, so that a temperature difference between the fluid and the wall is formed. As a result of the temperature difference, there is heat flow caused by the fluid in the wall through which the wall temperature slowly adjusts the fluid temperature. This method was proposed by [13]

Figure 1 shows the temperature distribution in the wall and the temporal course for various heat transfers when using the transient liquid crystal method. In the case of a pure heat transfer experiment without film cooling is now the heat transfer coefficient in the region observed from Fourier's theorem experience, assuming one-dimensional heat conduction and constant physical properties are determined using the boundary conditions and assuming a semi-infinite wall results the following equation.

In a film cooling experiment comes as a further variable the supplied through the holes cooling air added. It is a three-temperature problem with the mainstream temperature T_h , cooling air temperature T_c and wall temperature T_w . In order defined by the cooling air induced local change of the main stream temperature into account, the adiabatic wall temperature is introduced. In the film cooling case, it is used as a reference temperature instead of the mainstream temperature. In order to change the above equation to:

$$\frac{T_w - T_i}{T_{aw} - T_i} = 1 - \exp\left[\frac{\alpha^2 \tau}{k\rho c}\right] \operatorname{erfc}\left[\frac{\alpha\sqrt{\tau}}{\sqrt{k\rho c}}\right] \quad 1$$

Using the definition of adiabatic film cooling effectiveness

$$\eta_{aw} = \frac{T_h - T_{aw}}{T_h - T_c} \quad 2$$

Resulting

$$T_w - T_i = \left[1 - \exp\left[\frac{h^2 \tau}{k\rho c}\right] \operatorname{erfc}\left[\frac{h\sqrt{\tau}}{\sqrt{k\rho c}}\right] \right] [(1 - \eta_{aw})T_h - T_i + \eta_{aw}T_c] \quad 3$$

Unknown quantities in the equation, in addition to the temperatures during the test are measured, only the two characteristic parameters α and η_{aw} .

DEDUCTION OF THE FILM COOLING EFFECTIVENESS AND HEAT TRANSFER COEFFICIENT

For determining the unknowns in the equation (3) h , and η_{aw} two more equations are needed. There are two different measurements at the same aero thermodynamically settings necessary [13]. To calculate h , and η_{aw} using the measured data and the material constants of the desired quantities, there are several ways to achieve this: [13] proposes attempts before using thermochromics liquid crystals (TLC) were two indications are measured. These are the achievement of the green and blue color. Another possibility is to carry out two experiments with a variation of the main current temperature.[14] And [15] propose two attempts before when varying the cooling air temperature. The first experiment is performed with $T_c < T_h$ and the second at $T_c \approx T_h$. [16] Investigated the influence of the variation of the cooling air temperature on the film cooling effectiveness. With the variation of the cooling air temperature either the blowing ratio, the impulse or velocity ratio was kept constant. The best agreement was found in a constant blowing ratio. The idea was taken up by [17] and implemented in a regression method for multiple tests. Since a "two-experimental" or "two-indication method" according to submissions of high measurement errors for h (up to 10%) and η_{aw} (up to 20%) is possible, propose a method with 5 attempts.

This means, of five experiments, five-time variation of the cooling air temperature is deduced a value for h , and η_{aw} . The nonlinear system of equations with five equations and two unknowns is first linearized and then solved using a regression method. Thereby, the measurement error of 6% and 10% can be reduced.

The linearization and determination of the unknowns can be done for example, with a Gauss-Newton method. Since the multi-test procedure is quite time-consuming, [18] undertook further studies in order to reduce the number of attempts. With constant main stream temperature and blowing ratio they have conducted eight tests at different cooling air temperatures and in each case determined from two of the required parameters. In this case, the result of the method of [17] presented a when a cooling air temperature just above the calibration temperature of the liquid crystals and was selected far above the hot gas temperature. Thus, in a calibration temperature of the liquid crystals, the temperatures were $T_{TLC} = 38^\circ\text{C}$ and a main current temperature $T_h = 56^\circ\text{C}$, 42°C and $T_{c1} = T_{c2} = 75^\circ\text{C}$ determined to be optimal. In this case, the result of [17] with the same accuracy is confirmed by [19]. The error could be reduced for $T_{c1} = 36^\circ\text{C}$ and $T_{c2} = 86^\circ\text{C}$.

EXPERIMENTAL SETUP

The test rig consists of a rectangular channel simulating the outer surface of the turbine blade and a perpendicularly arranged square channel representing an internal blade cooling passage. Five angled film cooling holes introduce the coolant from the internal passage into the main flow (Figure 2). The dimensions of the channels and further

geometrical data can be found below (Table 1). The channels are both operated in sucking mode being connected to a vacuum pump. Both channels are equipped with two valves to adjust pressure and mass flow independently. Wire-screen heaters ensure the transient heating of the hot gas and coolant flow to the desired temperatures within less than one second.

They are designed to ensure a uniform and steady temperature distribution throughout the transient experiment. The hot gas channel heater is fitted with 11 serial mounted screens supplied by a 27 kW co-current flow. The coolant channel has three serial mounted screens with a maximum power input of 3 kW. To produce uniform boundary layer conditions in the hot gas channel a trip wire is positioned at before the row of holes. The test section starts at the row of holes and continues to in stream-wise direction. Figure 3 provides a detailed view of the arrangement of the cylindrical holes and some definition of variables.

The Reynolds number of the hot gas channel is determined from the total and static pressure using a Pitot tube. The Reynolds number refers to the coolant hole diameter (i.e. $d=5$ mm). The pressure tabs from the tube as well as the one from the coolant channel (see Figure 1) were connected to a different pressure measurement device (DSAENCL 3000, Scanivalve Corporation).

The temperatures were measured using K-Type thermocouples (Omega, 5SRTC-TT-KI-40-2M) combined with a data acquisition unit (Agilent 34970A) at a frequency of 0.104Hz. One of the thermocouple is positioned in the middle of the hot gas channel 20d ahead of the cooling holes and one in the middle of the coolant channel positioned underneath the row of holes (Figure 1).

The coolant channel mass flow and the Reynolds number were determined using laminar flow elements (LFE). The Reynolds number refers to the hydraulic diameter of the channel. By positioning one LFE before and one after the cooling holes, the jet mass flow and thus the blowing and momentum ratio could be deduced. The bottom of the hot gas Perspex channel is fully covered with black paint (Hallcrest Black Backing BB-G1) to intensify the contrast. Narrow band liquid crystals are applied to the surface using an airbrush system (Hallcrest TLC R38C1W). Before running the tests the liquid crystals were calibrated and a respective temperature of 38.1° C. The change of the liquid crystal color is then digitally recorded using a CCD camera (Sony DXC-390P 3CCD Color Camera 1/3") combined with a 15 mm lens (Fujinon 3CCD, 15 mm) at a spatial resolution of 576 x 720 and a frame rate of 25Hz.

TEST PROCEDURE

As discussed previously, for each test setup four experiments at different coolant temperatures are performed. At each temperature the Reynolds number of the cooling channel and the blowing ratio need to be readjusted using the valves. As mentioned before, the lowest coolant temperature was roughly set at the calibration level of the TLC as suggested by [18]. The highest temperature was framed by the demand of having at least four seconds test duration to minimize errors induced by the temporal resolution. The two remaining were conducted at coolant temperatures in between these boundaries.

A transient test is initiated by switching on the two wire-screen heater. Simultaneously the CCD-camera starts to record images of the TLC coated surface of the test section. The temporal temperature pattern is recorded for the data acquisition unit as well as the flow conditions (e.g. M , I , pc/ph). All experiments conducted for this study are conducted at constant hot gas channel Reynolds number. For each setup, four experiments are carried out (CHSA1 to CHSA4). Flow parameters are listed in Table 2.

After the completion of all experiments the recorded videos are analyzed for the lap time of TLC changing from the color-less to green at every pixel in the viewing domain. This and the records of, and the initial temperature can be then used to solve Equation 3 using a Gauss-Newton method in combination with a linear regression as discussed above

RESULTS AND DISCUSSIONS

Figure 4 shows the comparison of the adiabatic film cooling effectiveness with comparative experiments with similar operating parameters. The main difference between the experiments is that the cooling holes in the comparative experiments are fed from a plenum. Compared with CHSA1 a good agreement is downstream from a value of $x/D > 5$. In the region close to the hole there are high deviations. This can be explained with the highest measurement uncertainty of all experiments in the region close to the hole. On the other hand, may be responsible for the altered shape of the cooling air supply. The film cooling effectiveness in CHSA4 runs from an $x / D > 5$ with a constant distance below the determined values in comparative studies. Overall, one can say that the results of the present experiments were slightly different from the literature data, the differences may be due to the uncertainty of the different experimental setups used. In Figure 4.b the results of heat transfer coefficient are shown. The curves yield qualitatively similar trends to the comparative experimental data. Quantitatively, a difference of about 20% is present. The trends are reproduced correctly in all curves. For these reasons, a comparison with literature data is limited.

The Figures (5, 6, and 7) show the local distribution of the heat transfer coefficient for smooth cooling air channel as contour plots, span-wise, and stream-wise distributions at different cooling air Reynolds numbers as listed in table 5.4. Figures Shows in all cases relatively widely differing distributions. In CHSA-1, the heat transfer is increased immediately downstream of the hole by more than two times. Further downstream it is reduced, and approximately remain the same until the end of the considered area. In addition, at a distance $x/D = 15$ downstream the hole, there is a visible divergent area of increased heat transfer (marked area in Figure 5.1). This is due to turbulence braids, which are formed from the cooling air stream and run divergent from each other. [22] Also was reported on this phenomenon. For high cooling air Reynolds number (CHSA-4S) there is a slight elevation on the heat transfer coefficient near the hole in the range ($0 < x/D < 8$), then the influence of the cooling air jets is no longer visible. Compared to CHSA-1S there is a clear reduction and a modified surface distribution over the entire measurement range. These observations are confirmed by the exposure of the span wise and stream wise plots. The Average plots comparison of the all cases is confirmed these observations (Figure 8). CHSA-1S shows an elevation directly behind the drill hole, the downstream decreases evenly. Overall, a more extensive distribution is observed. In contrast, in the CHSA-4S it can be seen a strong reduction of the heat transfer coefficient along the center line of the holes.

The local distribution of the adiabatic film cooling effectiveness of different cooling air Reynolds number is shown in Figures, and. The cooling jets are adjacent, and the film cooling effectiveness decreases immediately after the hole monotonically. The local distributions show predominantly symmetrically disposed adjacent cooling air jets. There are hardly any differences apparent in the comparison of the individual holes. Also, the beam is not deflected by the right-angle flow in the cooling channel after the outlet from the hole. CHSA- shows a higher adiabatic film cooling effectiveness directly downstream of the hole in the region $0 < x/D < 15$.

CONCLUSIONS

Experimental investigation is performed to investigate film cooling performance with transient liquid crystal

technique. Experiments are performed at different flow conditions of cooling air and the results show the following:-

- Liquid crystal transient method is an effective technique for measuring film cooling performance
- The present experimental results of film cooling performance for CHSA are compared and well confirmed by the results from previous researches.
- For CHSA, the increase in the cooling air Reynolds number has a drop in the heat transfer coefficient result
- For CHSA, uniform film cooling effectiveness in the lateral direction through the different holes is maintained axis-symmetric for all flow rates.
- In the adiabatic film cooling effectiveness, there is a monotonic increase in all rib configurations for all Blowing Ratio.
- The increase in the Blowing Ratio leads to an increase of heat transfer to the surface. In the region near to the hole exit, however, the beam tends to replace at all considered Blowing Ratios. This effect becomes more intense with increasing Blowing Ratio. Consequently, for low Blowing Ratios partially near the hole there is a higher heat transfer coefficient and at further downstream there is a lower heat transfer coefficient. Similarly, the results of the adiabatic film cooling effectiveness showed their dependency on the Blowing Ratio. An increase in the Blowing Ratio does not necessarily lead to increased efficiency.
- For Blowing Ratios ($M \geq 1.5$) there is an area formed between the holes in which increased heat transfer coefficient and adiabatic film cooling effectiveness, whereas these values decreased along the hole axis. The area formed between the holes is explained by the fact that the adjacent kidney vortices formed from the cooling air jets enhanced transport cooling air from both directions on the surfaces between the holes.

REFERENCES

1. GOLDSTEIN, R.J.: Film Cooling. In: *Advances in Heat Transfer*, Irvine T.F. and J.P. Hartnett Eds. Academic Press, San Diego 7 (1971), S.321–379.
2. GOLDSTEIN, R.J.; ECKERT, E.R.G.; BURGGRAF, F.: Effects of Hole Geometry and Density on Three-Dimensional Film Cooling. In: *International Journal of Heat and Mass Transfer* 17 (1974), S.559–607.
3. BUNKER, R.S.: A Review of Shaped Hole Turbine Film-Cooling Technology. In: *ASME Journal of Heat Transfer* 127 (2005), S.441–453.
4. LALETIN, P.; WEIGAND, B.; BETTELINI, M.; WOLFERSDORF, J. Von: 3D Numerical Simulation of Film Cooling with Fan Shaped Holes on a Flat Plate. In: *3rd Baltic Heat Transfer Conference, Gdansk, Poland (1999)*.
5. HAVEN, B.A.; KUROSAKA, M.: Improved Jet Coverage through Vortex Cancellation. In: *AIAA Journal* 34 (1997), No.11, S.2443–2444.
6. HAVEN, B.A.; KUROSAKA, M.: Kidney and Anti-Kidney Vortices in Jet Crossflow. In: *Journal of Fluid Mechanics* 352 (1997), p.27–64.
7. LUTUM, E.; JOHNSON, B.V.: Influence of the hole Length-to-Diameter Ratio on Film Cooling with Cylindrical Holes. In: *ASME Journal of Turbomachinery* 121 (1999), p.209–216.

8. GRITSCH, M.; SAUMWEBER, C.; SCHULZ, A.; WITTIG, S.; SHARP, E.: Effect of Internal Coolant Crossflow Orientation on the Discharge Coefficient of Shaped Film Cooling Holes. In: *ASME Journal of Turbomachinery* 122 (1999), S.146–152.
9. GRITSCH, M.; SAUMWEBER, C.; SCHULZ, A.; WITTIG, S.; SHARP, E.: Effect of Internal Coolant Crossflow Orientation on the Discharge Coefficient of Shaped Film Cooling Holes. In: *ASME Journal of Turbomachinery* 122 (1999), S.146–152.
10. BRUNDAGE, A.L.; PLESNIAK, M.W.; RAMADHYANI, S.: Influence of Coolant Feed Direction and Hole Length on Film Cooling Jet Velocity Profiles. In: *ASME Paper 99-GT-35* (1999).
11. WILFERT, G.; LIEBE, R.: Vorrichtung und Verfahren zur Kühlung einer einseitig von Heissgas umströmten Wand. *Europäische Patentanmeldung EP0990772A2*. 1999.
12. LEYLEK, J.H.; ZERKLE, R.D.: Discrete-Jet Film Cooling: A Comparison of Computational Results with Experiments. In: *ASME Journal of Turbomachinery* 116 (1994), p.358–368.
13. VEDULA, R.J.; METZGER, D.E.: A Method for the Simultaneous Determination of Local Effectiveness and Heat Transfer Distributions in Three-Temperature Convection Situations. In: *ASME Paper 91-GT-345* (1991).
14. EKKAD, S.V.; HAN, J.C.: A Transient Liquid Crystal Thermography Technique for Gas Turbine Heat Transfer Measurements. In: *Meas.Sci.Technology* 11 (2000), S.957–968.
15. YU, Y.; YEN, C.H.; SHIH, T.I.P.; CHYU, M.K.; GOGINENI, S.: Film Cooling Effectiveness and Heat Transfer Coefficient Distributions around Diffusion Shaped Holes. In: *ASME Journal of Heat Transfer* 124 (2002), p.820–827.
16. LIGRANI, P.M.; CAMCI, C.: Adiabatic Film Cooling Effectiveness from Heat Transfer Measurements in Compressible Variable Property Flow. In: *ASME Journal of Heat Transfer* 107 (1985), p.313–320.
17. DROST, U.; BOELCS, A.; HOFFS, A.: Utilization of the Transient Liquid Crystal Technique for Film Cooling Effectiveness and Heat Transfer Investigations on a Flat Plate and a Turbine Airfoil. In: *ASME Paper 97-GT-26* (1997).
18. AI, D.; DING, P.P.; CHEN, P.H.: The Selection Criterion of Injection Temperature Pair for Transient Liquid Crystal Thermography on Film Cooling Measurements. In: *International Journal of Heat and Mass Transfer* 44 (2001), S.1389–1399.
19. KISSEL, H.P.; WEIGAND, B.; WOLFERSDORF, J. Von; NEUMANN, S.O.; UNGE-WICKELL, A.: An Experimental and Numerical Investigation of the Effect of Cooling Channel Crossflow on Film Cooling Performance. In: *ASME Paper GT2007-27102* (2007).
20. COLEMAN, H.W.; STEELE, W.G.: *Experimentation and Uncertainty Analysis for Engineers*. Wiley, New York, 1999.
21. YU, Y.; YEN, C.H.; SHIH, T.I.P.; CHYU, M.K.; GOGINENI, S.: Film Cooling Effectiveness and Heat Transfer Coefficient Distributions around Diffusion Shaped Holes. In: *ASME Journal of Heat Transfer* 124 (2002), p.820–827.

22. MAYHEW, J.E.: An Experimental Investigation of the Effect of Freestream Turbulence on Film Cooling using Thermochromics Liquid Crystal Thermography, University of California, Davis, Dissertation, 1999.
23. THOLE, K.; GRITSCH, M.; SCHULZ, A.; WITTIG, S.: Flow field Measurements for Film-Cooling Holes with Expanded Exits. In: ASME Journal of Turbomachinery 120 (1998), p.327–336.

APPENDIES

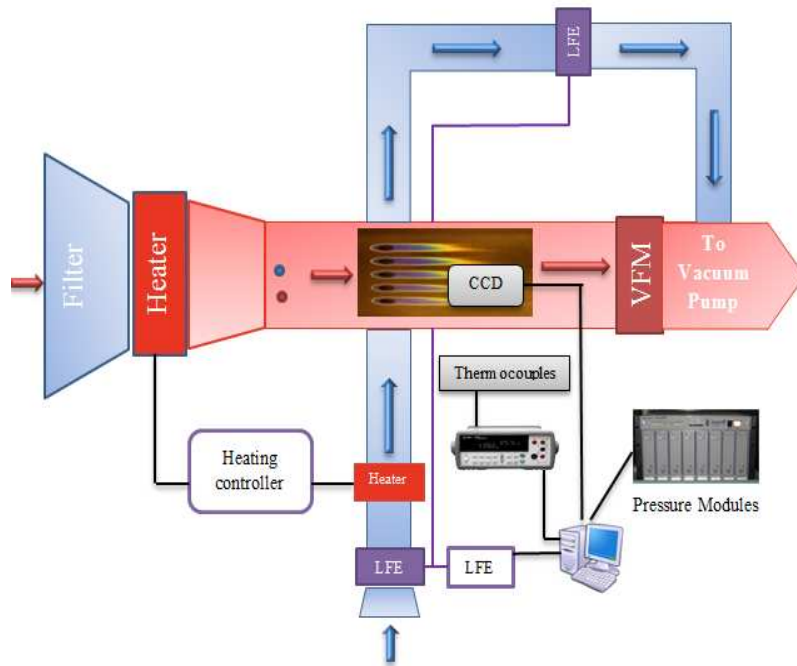


Figure 1: Experimental Setup Interfaces

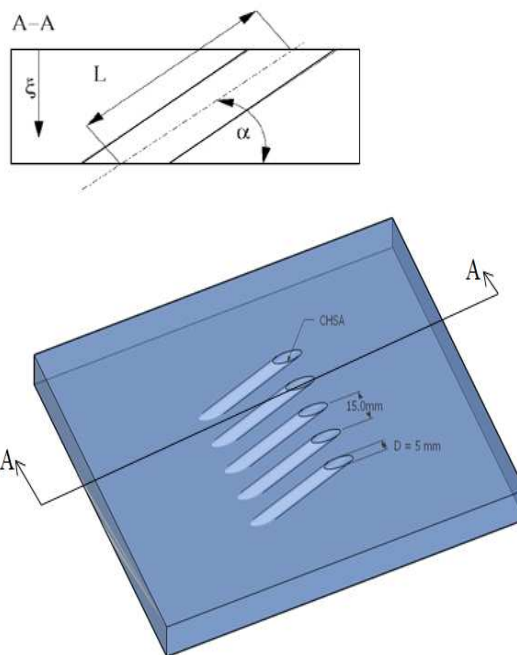


Figure 2: Geometry of the (CHSA) Film Cooling Hole

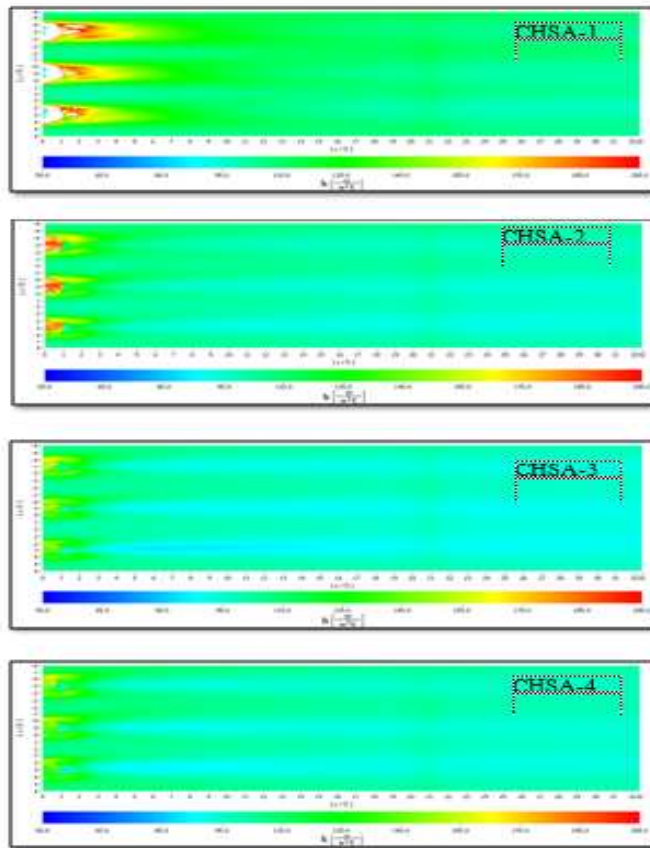


Figure 3: Heat Transfer Contour Plots for $M=0.5$ and Different $Re_{Dh,c}$.

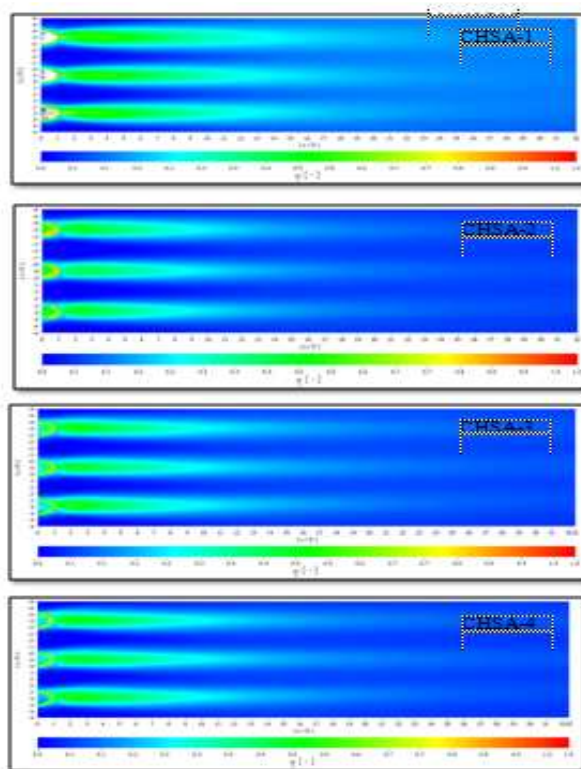


Figure 4: Adiabatic Film Cooling Effectiveness Contour Plots for $M=0.5$ and Different $Re_{Dh,c}$.